

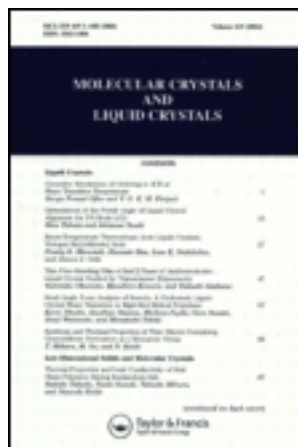
This article was downloaded by: [University of Haifa Library]

On: 17 August 2012, At: 10:20

Publisher: Taylor & Francis

Informa Ltd Registered in England and Wales Registered Number: 1072954

Registered office: Mortimer House, 37-41 Mortimer Street, London W1T 3JH, UK



Molecular Crystals and Liquid Crystals Science and Technology. Section A. Molecular Crystals and Liquid Crystals

Publication details, including instructions for authors and subscription information:

<http://www.tandfonline.com/loi/gmcl19>

Electron Paramagnetic Resonance and LIESST Effect in Spin-Crossover Cis-Bis(Thiocyanato)Bis[N-(2-Pyridyl-Methylene)Aminobiphenyl]Iron(II) Compound

Jean-François Létard^a, Hervé Daubric^b,
Christophe Cantin^b, Janis Kliava^b, Yacine A.
Bouhedja^a, Olivier Nguyena^a & Olivier Kahn^a

^a Laboratoire des Sciences Moléculaires, Institut de Chimie de la Matière Condensée de Bordeaux, UPR CNRS 9048, 33608, Pessac, Cedex, France

^b Centre de Physique Moléculaire Optique et Hertzienne, UMR Université, Bordeaux I-CNRS 5798, 351 cours de la Libération, 33405, Talence, Cedex, France

Version of record first published: 24 Sep 2006

To cite this article: Jean-François Létard, Hervé Daubric, Christophe Cantin, Janis Kliava, Yacine A. Bouhedja, Olivier Nguyena & Olivier Kahn (1999): Electron Paramagnetic Resonance and LIESST Effect in Spin-Crossover Cis-Bis(Thiocyanato)Bis[N-(2-Pyridyl-Methylene)Aminobiphenyl]Iron(II) Compound,

To link to this article: <http://dx.doi.org/10.1080/10587259908028891>

PLEASE SCROLL DOWN FOR ARTICLE

Full terms and conditions of use: <http://www.tandfonline.com/page/terms-and-conditions>

This article may be used for research, teaching, and private study purposes. Any substantial or systematic reproduction, redistribution, reselling, loan, sub-licensing, systematic supply, or distribution in any form to anyone is expressly forbidden.

The publisher does not give any warranty express or implied or make any representation that the contents will be complete or accurate or up to date. The accuracy of any instructions, formulae, and drug doses should be independently verified with primary sources. The publisher shall not be liable for any loss, actions, claims, proceedings, demand, or costs or damages whatsoever or howsoever caused arising directly or indirectly in connection with or arising out of the use of this material.

Electron Paramagnetic Resonance and LIESST Effect in Spin-Crossover *Cis-Bis(Thiocyanato)Bis[N-(2-Pyridyl-Methylene)Aminobiphenyl]Iron(II) Compound*

JEAN-FRANÇOIS LÉTARD^a, HERVÉ DAUBRIC^b,
CHRISTOPHE CANTIN^b, JANIS KLIAVA^b, YACINE A. BOUHEDJA^a,
OLIVIER NGUYEN^a and OLIVIER KAHN^a

^aLaboratoire des Sciences Moléculaires, Institut de Chimie de la Matière
Condensée de Bordeaux, UPR CNRS 9048, 33608 Pessac Cedex, France and

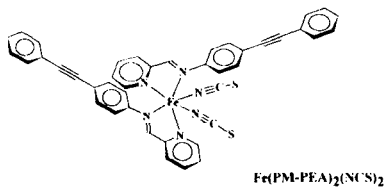
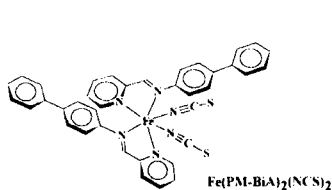
^bCentre de Physique Moléculaire Optique et Hertzienne, UMR Université
Bordeaux I-CNRS 5798, 351 cours de la Liberation, 33405 Talence Cedex, France

Two different phases of spin-crossover *cis-bis*(thiocyanato)-*bis*(N-2'-pyridylmethylene)-4-(aminobiphenyl) iron(II), $\text{Fe}(\text{PM-BiA})_2(\text{NCS})_2$ have been investigated by EPR in X- and Q-bands. The EPR parameters for Mn^{2+} show that the phase II has similar behavior to intentionally doped compound. EPR spectra as function of the temperature reveal that the spin transition of the iron(II) centers induced some modifications on the whole structure and then on the environment of the manganese ions. The LIESST effect is reported for the two phases and for $\text{Fe}_{0.216}\text{Mn}_{0.784}(\text{PM-BiA})_2(\text{NCS})_2$. The magnetic properties under irradiation of the phase II and of $\text{Fe}_{0.216}\text{Mn}_{0.784}(\text{PM-BiA})_2(\text{NCS})_2$ are very similar and the limit temperature of the HS metastable state is around $T_{\text{liesst}} = 50$ K, as compared to 80 K for the phase I. The new kind of bistability called LITH (Light Induced Thermal Hysteresis) has been observed for the three derivatives. The $\text{HS} \rightarrow \text{LS}$ relaxation is higher for the phase II and $\text{Fe}_{0.216}\text{Mn}_{0.784}(\text{PM-BiA})_2(\text{NCS})_2$ than for the phase I.

Keywords: Electron Paramagnetic Resonance; Spin-crossover; Bistability

INTRODUCTION

In iron(II) coordination compounds spin conversion from a low-spin (LS, $S = 0$) state to a high-spin (HS, $S = 2$) state has been the subject of many studies during the last three decades. Spin transition can be induced by a change of temperature or pressure and or by light irradiation.¹ Recently, the use of such materials as molecular-based memory devices and displays has been suggested.² In fact, several iron(II) derivatives show a bistability : the LS to HS transition occurs at a higher temperature than the HS to LS transition, forming a thermal hysteresis loop. In this event, a number of questions must be answered, concerning structural modifications accompanying the spin transition. Recently, we have synthesized strongly cooperative spin-crossover assemblies of mononuclear molecules, based on strong interactions through the stacking of aromatic rings. Along this line, we already reported two mononuclear spin-crossover derivatives ; i) *cis*-bis(thiocyanato)bis(*N*-2'-pyridylmethylene)-4-(phenylethynyl)aniline iron(II), $\text{Fe}(\text{PM-PEA})_2(\text{NCS})_2$, with a very large hysteresis as well as relatively high temperatures of transition: $T_{1/2\downarrow} = 194 \text{ K}$, $T_{1/2\uparrow} = 231 \text{ K}$ ³ and ii) *cis*-bis(thiocyanato)bis(*N*-2'-pyridylmethylene)-4-(aminobiphenyl) iron(II), $\text{Fe}(\text{PM-BiA})_2(\text{NCS})_2$ which undergoes an unusually abrupt transition with a very narrow and sharp hysteresis: $T_{1/2\downarrow} = 168 \text{ K}$, $T_{1/2\uparrow} = 173 \text{ K}$.⁴ The crystal structure of $\text{Fe}(\text{PM-BiA})_2(\text{NCS})_2$ solved both at room temperature (HS state) and at 140 K (LS state) shows that the space group is not changed during the spin transition (orthorhombic *Pccn*) and that the main structural feature is the reorganization of the FeN_6 core toward a more regular octahedron in the LS state.^{4,6} Recently, we have reported the LIESST (Light-Induced Excited Spin State-Trapping) in $\text{Fe}(\text{PM-BiA})_2(\text{NCS})_2$ recorded at 10 K within a SQUID cavity.⁴ A slow rate of quantum mechanical tunneling from the metastable HS state to the LS state has been observed and the limit temperature was estimated around 80 K. This behavior is correlated with an



unusually large change in Fe-N(organic ligand) bond lengths in the course of the spin transition.

Meanwhile for $\text{Fe}(\text{PM-BiA})_2(\text{NCS})_2$ depending on the synthetic method, a second phase can be obtained, exhibiting a complete and gradual spin transition with $T_{1/2\downarrow} = 205 \text{ K}$ and $T_{1/2\uparrow} = 209 \text{ K}$.⁵ Up to now, single crystal of phase II has not been obtained. A powder diffraction showed that at room temperature the best cell was obtained with a monoclinic phase ($P2_1/c$).⁴ In the present work, we report the EPR spectra of the phases I and II. A direct observation of spin transitions in iron(II) compounds by EPR is difficult, if not impossible, since the Fe^{2+} ion is "EPR silent" not only in the LS *diamagnetic* state, but, in practice, also in its HS *paramagnetic* state because of a very short spin-lattice relaxation time and/or a very large zero-field splitting.⁷ The spin transition experienced by the Fe^{2+} ions can however be detected by EPR in an *indirect* way, from an analysis of modifications of EPR spectra of some foreign paramagnetic ions doped in the spin-transition compound. Up to now, two foreign paramagnetic ions have been systematically used in the EPR studies of iron(II) spin crossover compounds, viz., $\text{Cu}^{2+}(3d^9)^{8-11}$ and $\text{Mn}^{2+}(3d^5)^{10-14}$.

We also present the magnetic properties of $\text{Fe}(\text{PM-BiA})_2(\text{NCS})_2$ doped with Cu^{2+} , Zn^{2+} and Mn^{2+} . The LIESST effect recorded at 10 K within a SQUID cavity for two naturally doped samples (phases I and II) and an intentionally doped with 21.6 % of manganese sample are compared. In fact, doping spin-transition compounds with foreign species can modify their characteristics (transition temperatures, hysteresis loop, critical temperature limit of LIESST effect...), which can be very interesting for potential applications.

EXPERIMENTAL SECTION

The phases I and II of $\text{Fe}(\text{PM-BiA})_2(\text{NCS})_2$ were found to be naturally doped with manganese ions. Elemental analysis performed by the Service Central d'Analyse (CNRS) in Vernaison (France) has shown a doping level of ca. 0.1 % Mn/Fe. Besides, intentionally doped compounds with 1 % and 21.6 % of Mn/Fe were prepared. Anal. Calcd. for $\text{Fe}_{0.99}\text{Mn}_{0.01}\text{C}_{38}\text{H}_{28}\text{N}_6\text{S}_2$: C, 66.28; H, 4.10; N, 12.20; S, 9.31; Fe, 8.03; Mn, 0.08. Found: C, 66.33; N, 12.17; Fe, 7.65; Mn, 0.10; Anal. Calcd. for $\text{Fe}_{0.216}\text{Mn}_{0.784}\text{C}_{38}\text{H}_{28}\text{N}_6\text{S}_2$: C, 66.29;

H, 4.10; N, 12.21; S, 9.32; Fe, 6.65; Mn, 1.44. Found: C, 66.23; N, 12.27; Fe, 6.83; Mn, 1.50.

Magnetic susceptibility measurements were carried out on powder samples (about 20 mg), over the temperature range 300–80 K, using a fully automatized Manics DSM-8 Faraday magnetometer equipped with a DN-170 Oxford Instruments continuous-flow cryostat and a BE 15f Bruker electromagnet operating at *ca.* 0.8 Tesla. Data were corrected for the magnetization of the sample holder and for diamagnetic contributions. The X-Band EPR spectra were recorded with a Varian V4502 spectrometer equipped with a Varian E257 variable temperature accessory operating in the range -185°C to 300°C . The Q-Band EPR spectra were recorded with a Bruker ESP300 spectrometer supplied with a ER4121 VT digital temperature control unit operating between 100 and 700 K.

RESULTS AND DISCUSSION

Magnetic behavior

Figure 1 shows the HS molar fraction (γ_{HS}) versus the temperature (T) of the samples of $\text{Fe}(\text{PM-BiA})_2(\text{NCS})_2$ intentionally doped with Mn^{2+} , Zn^{2+} and Cu^{2+} in phases I and II.

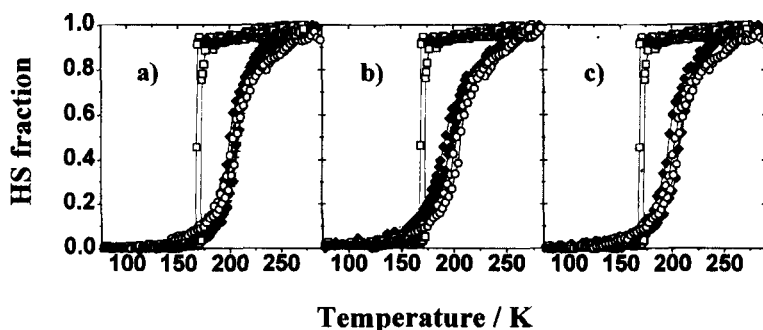


Figure 1. $\text{Fe}(\text{PM-BiA})_2(\text{NCS})_2$ in ($\square \square \square$) phase I and ($\circ \circ \circ$) phase II and $\text{Fe}_{1-x}\text{M}_x(\text{PM-BiA})_2(\text{NCS})_2$ with (a) ($\blacklozenge \blacklozenge \blacklozenge$) $x = 0.01$ and ($+++$) $x = 0.21$ of Mn/Fe; (b) ($\blacklozenge \blacklozenge \blacklozenge$) $x = 0.1$ of Zn/Fe and (c) ($\blacklozenge \blacklozenge \blacklozenge$) $x = 0.001$ of Cu/Fe.

In all cases, the $\gamma_{HS}(T)$ curves were deduced from the magnetic susceptibility measurements as $\chi_M T / [(\chi_M T)_{HT}]$, where $\chi_M T$ is the molar magnetic susceptibility at a temperature T and $(\chi_M T)_{HT}$ is the high-temperature limit of $\chi_M T$. The $\gamma_{HS}(T)$ curves of intentionally doped compounds are similar to those of phase II of $\text{Fe}(\text{PM-BiA})_2(\text{NCS})_2$. The spin transition is complete and gradual, and successive thermal cycles do not modify the thermal hysteresis loop.

EPR spectra

We only present the EPR spectra of the Mn^{2+} ions due to the fact that i) both phases (I and II) of $\text{Fe}(\text{PM-BiA})_2(\text{NCS})_2$ show typical spectra and ii) the investigation of intentionally doped compound with Cu^{2+} reveals only some residual traces in X- and Q-bands at low temperature where the iron center is in LS state. The EPR spectra in X-band ($\nu = 9.317 \text{ GHz}$) and in Q-band ($\nu = 34 \text{ GHz}$) of phase I are presented in Figure 2 as a function of temperature.

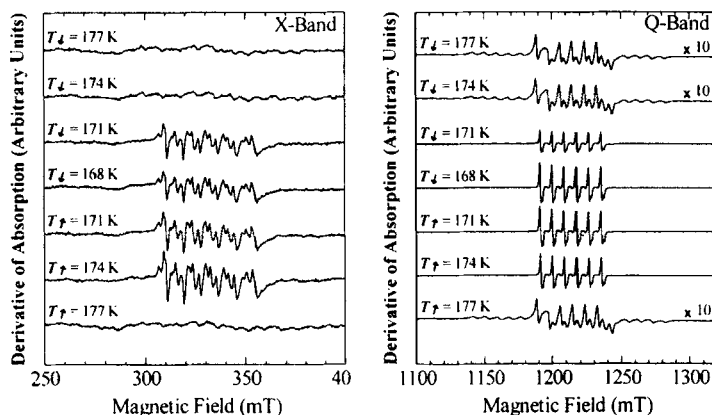


Figure 2. X- and Q-bands EPR spectra of the naturally doped $\text{Fe}(\text{PM-BiA})_2(\text{NCS})_2$ in phase I in the warming (T_{\uparrow}) and cooling (T_{\downarrow}) modes.

The EPR spectra change slightly from room temperature down to 174 K, then a pronounced change occurs in the region 174 - 168 K. At lower temperature EPR spectra remain almost constant. In the warming mode a similar behavior is observed; from 100 to 171 K the spectra do not

appreciably change, then around 171 - 177 K some transformations occur and at higher temperature the EPR spectra remain nearly identical. For the phase II, EPR spectra have been observed only in Q-band (figure 3). The absence of X-band EPR spectra seems to indicate a very low concentration of Mn^{2+} ions. From room temperature down to 130 K a continuous transformation of the EPR spectra have been recorded ; at 290 K

the spectra are constituted of six broad bands, whereas at 130 K some slight lines structure appear. The EPR spectra recorded for intentionally doped compound $Fe_{0.99}Mn_{0.01}$ in X- and in Q-bands are shown in figure 4.

Figure 3. Q-band EPR spectra of the naturally doped $Fe(PM-BiA)_2(NCS)_2$ in phase II in the warming ($T \uparrow$) mode.

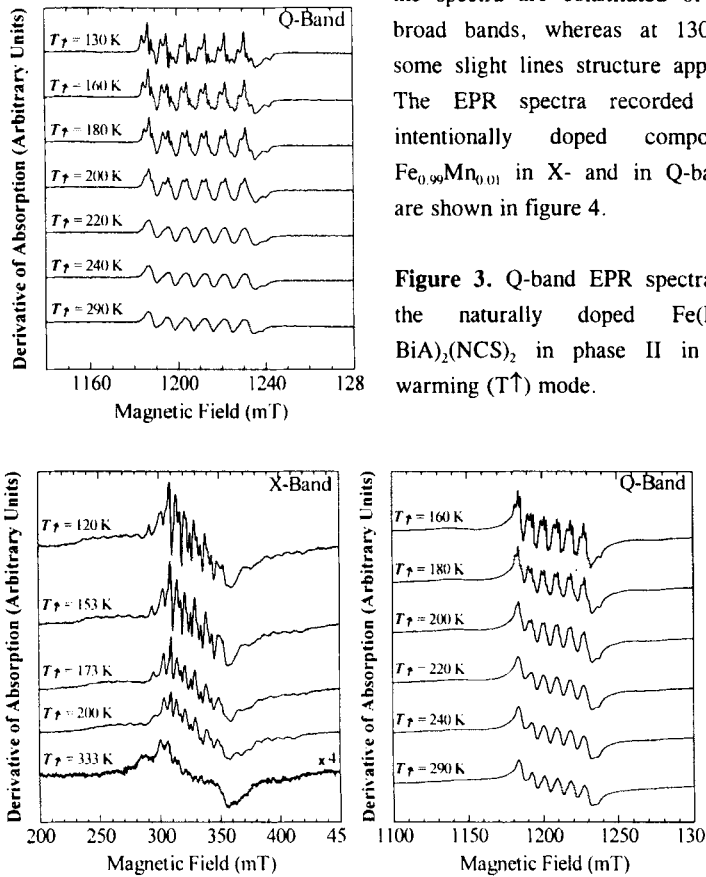


Figure 4. X- and Q-bands EPR spectra of the intentionally doped $Fe_{0.99}Mn_{0.01}(PM-BiA)_2(NCS)_2$.

The EPR spectra of Mn^{2+} ions in a powder system can be described by the orthorhombic spin Hamiltonian (eq. 1), where $g \approx g_r = 2.0023$, $S = 5/2$ and $I = 5/2$. The g -factor and the hyperfine structure (hfs) constant A for Mn^{2+} are isotropic with a good accuracy. For the $g = 2.0$ centres the condition $|D|, |E|, |A| \ll g\beta B$ holds. The presence of the fine structure (fs) terms in equation 1 gives rise to five "allowed" fs multiplets $\langle M = \pm 5/2 | \leftrightarrow \langle M = \pm 3/2 |$, $\langle M = \pm 3/2 | \leftrightarrow \langle M = \pm 1/2 |$ and $\langle M = -1/2 | \leftrightarrow \langle M = +1/2 |$. Meanwhile, for comparable absolute values of fs and hfs parameters, the selection rules governing the intensities of various hfs transitions are broken down, so that each fs multiplet, besides six "allowed" hfs components, $m = \pm 5/2, \pm 3/2, \pm 1/2$, $\Delta m = 0$, features a number of "forbidden" hfs components with $\Delta m = \pm 1, \pm 2, \dots, \pm 5$.

$$\mathcal{H} = g\beta B \cdot S + D \left[S_z^2 - \frac{1}{3} S(S+1) \right] + E (S_x^2 - S_y^2) + AS \cdot I \quad (\text{eq. 1})$$

In X-band the EPR spectra of phase I (figure 2) are resolved only for hfs components of the central fs multiplet, $\langle M = -1/2 | \leftrightarrow \langle M = +1/2 |$ at low temperature where the Fe^{2+} ions are in LS state, whereas in the HS state of Fe^{2+} the resolution of the hfs components is lost. In Q-band a quite well resolved EPR spectrum is observed already at room temperature (figs. 2-4). The improvement of resolution in the Q-band spectra can be explained by the form of the expression of the resonance magnetic field B_r for a central fs transition $\langle -1/2, m | \leftrightarrow \langle +1/2, m + \Delta m |$ (eq. 2) calculated to third order in perturbation theory.¹⁵

$$g\beta B_r = g\beta B_0(m, \Delta m) + \frac{16}{g\beta B_i} (|\lambda|^2 - 2|\rho|^2) - (2m + \Delta m) \frac{8A}{(g\beta B_i)^2} (9|\lambda|^2 - 2|\rho|^2) - (2m + \Delta m)(1 + \Delta m) \frac{4A^2}{(g\beta B_i)^2} \sigma \quad (\text{eq. 2})$$

where

$$g\beta B_0(m, \Delta m) = h\nu - (2m + \Delta m) \frac{A}{2} + [(2m + \Delta m)^2 + (17 - \Delta m)^2 - 324] \frac{A^2}{8g\beta B_i} - [4(m + \Delta m)^3 + 4m^3 - (2m + \Delta m)(65 + 134\Delta m)] \frac{A^3}{16(g\beta B_i)^2}$$

$$|\lambda|^2 = \sin^2 \vartheta [(D + E \cos 2\varphi)^2 \cos^2 \vartheta + E^2 \sin^2 2\varphi]$$

$$|\rho|^2 = \{ [D \sin^2 \vartheta - E(1 + \cos^2 \vartheta) \cos 2\varphi]^2 + 4E^2 \cos^2 \vartheta \sin^2 2\varphi \} / 16$$

$$\sigma = [D(3 \cos^2 \vartheta - 1) - 3E \sin^2 \vartheta \cos 2\varphi] / 2$$

The width of the resonance features in a powder EPR spectrum is mainly due to angular variations of their resonance fields. In passing from X- to Q-bands, the central lines of fs transition are narrowed approximately in proportion to the ratio of resonance frequencies of the two bands. The increase of the lateral parts resolution of the X-band (figure 2) in the HS state ($T \downarrow = 174$ K) in regard to the LS state ($T \uparrow = 174$ K), can not be explain by a simple line broadening caused by spin-spin interactions between Mn^{2+} and paramagnetic HS Fe^{2+} ions or by a fast spin-lattice relaxation of the latter ions. It seems that the key factors to explain such transformations could be an indication of a structural transformation in the environment of the Mn^{2+} during the spin transition of the Fe^{2+} ion.

In order to get a more quantitative insight in this transformation, simulations of the EPR spectra in the LS and HS states of Fe^{2+} have been carried out. The laboratory-developed simulation program takes into account all "allowed" fs and both "allowed" and "forbidden" hfs components. Their intensities are determined using the Bir's method,¹⁶ with W the transition intensity averaged over all directions of the microwave magnetic field and F the lineshape, with an orientation-dependent linewidth ΔB , including broadening due to spin-lattice and spin-spin interactions as well as to static disorder¹⁵ (eq. 3). The notations ϑ and φ are the polar and azimuthal angles of the directing magnetic field B with the axes of the spin Hamiltonian (eq. 1) and ν is the frequency of the microwave magnetic field.

$$\mathcal{P}(B) = \sum_{i=1}^{2N} \sum_{j=1}^{2l+1} \sum_{k=-2l}^{2l} \int_0^{2\pi} \int_0^{\pi} W(D, E, \vartheta, \varphi) \left| \frac{dB_i}{d\nu} \right| F[B - B_i(D, E, \vartheta, \varphi), \Delta B] \sin \vartheta d\vartheta d\varphi \quad (\text{eq. 3})$$

Figure 5 presents a comparison between experimental and best-fit computer-simulated EPR spectra for the naturally doped sample in phase I. The best-fit EPR parameters for Mn^{2+} ions in Q- and X-bands are listed in Table 1 for the two phases and for the intentionally doped compound. The good accuracy of the fits between the experimental and the computer-simulated EPR spectra and the similar parameters obtain by the fit of the Q- and X-bands provide to us some confidence in the description of the EPR spectra.

Table 1. Best-fit EPR parameters for Mn^{2+} ions in Q- and X-band. The numbers in parenthesis are the standard errors.

	Naturally doped samples (0.1 % Mn/Fe)					Intentionally doped sample	
	Phase I			Phase II		(1 % Mn/Fe)	
	$T \uparrow = 174 \text{ K}$ (LS)		$T \downarrow = 174 \text{ K}$ (HS)	$T = 130 \text{ K}$ (LS)	$T = 290 \text{ K}$ (HS)	$T = 160 \text{ K}$ (LS)	$T = 290 \text{ K}$ (HS)
	X-band	Q-band	Q-band	Q-band	Q-band	Q-band	Q-band
g	2.000(3)	2.000(3)	2.000(3)	2.000(3)	2.000(3)	2.000(3)	2.000(3)
A (10^{-4} cm^{-1})	-82(1)	-82(1)	-82(1)	-82(1)	-82(1)	-82(1)	-82(1)
D (10^{-4} cm^{-1})	165(5)	162(5)	418(5)	415(10)	310(5)	385(10)	310(5)
E (10^{-4} cm^{-1})	55(5)	53(5)	17(5)	105(10)	75(5)	95(10)	80(5)
λ ($= E/D$)	1/3	1/3	1/25	1/4	1/4	1/4	1/4

From Table 1, it is seen that the g and A values remain constant during the spin transition, respectively 2.0 ± 0.003 and $-82 \pm 1 \cdot 10^{-4} \text{ cm}^{-1}$, whereas the fs parameters (D and E) change significantly. The calculated ratio λ ($= E/D$) shows that for the phase I, the Mn^{2+} ions are subject to maximal degree in rhombic distortion ($\lambda \approx 1/3$) when the Fe^{2+} center is in LS state, whereas a quasi-axial symmetry ($\lambda \approx 1/25$) is obtain when Fe^{2+} is in HS state. The axial fs parameter D in the HS state almost three times larger than in the LS state of Fe^{2+} reveals a strong axial distortion arising at the Mn^{2+} sites in the HS state of Fe^{2+} ions. For the phase II and the intentionally doped sample, the λ -parameter (1/4) of the HS state indicates more rhombic distortions of Mn^{2+} ions than for the phase I (1/25). The structures of the phases I and II are very different.

The EPR spectra show that in the course of the spin conversion of the iron(II) centers the environment of the manganese ions are strongly modified. Two reasons for such modifications can be envisaged; i) some

spin-spin interactions between Mn^{2+} ($S = 5/2$) foreign ions and Fe^{2+} ions in HS state and ii) some structural change in the course of the spin transition. The former reason can be excluded in a first hypothesis due to the fact that in the crystal structure both in HS and LS states of $\text{Fe}(\text{PM-BiA})_2(\text{NCS})_2$ the metal-metal distances are around 10 Å.^{4,6} Thus, we can conclude that any structural changes accompanying the spin transition are sure short-range ones (inside the Fe^{2+} complex) but also long-range ones involving the whole structure. Such modifications are in contrast with the previous results obtained for triazole-based compounds where only a rather moderate line broadening has been observed in the HS state of Fe^{2+} .⁹

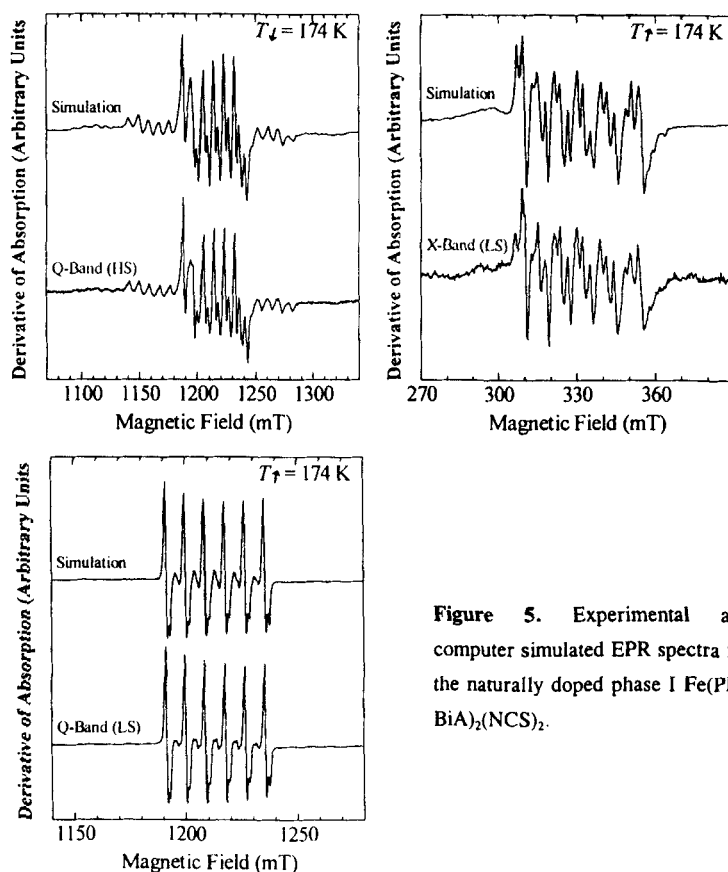


Figure 5. Experimental and computer simulated EPR spectra for the naturally doped phase I $\text{Fe}(\text{PM-BiA})_2(\text{NCS})_2$.

LIESST effect

The LIESST experiments were carried out on the powder sample of the $\text{Fe}(\text{PM-BiA})_2(\text{NCS})_2$ in phases I and II, as well as for the $\text{Fe}_{0.216}\text{Mn}_{0.784}(\text{PM-BiA})_2(\text{NCS})_2$. A typical experiment is shown in Figure 6. The sample is first slowly cooled from ca. 100 K down to 10 K, and the $\chi_{\text{M}}T$ versus T curve confirms that Fe^{2+} ions are in LS state. At 10 K, the sample is then irradiated (mode ON) with a red light ($\lambda = 647.1 - 676.4 \text{ nm}$) for one hour with an intensity of 50 mW; $\chi_{\text{M}}T$ was found to increase rapidly, then to reach a value of ca. $0.7 \text{ cm}^3 \text{ K mol}^{-1}$, indicating a partial conversion ($\approx 20 \%$) of the LS state into the HS state, according to the well-known LIESST process.¹⁷

Without further irradiation (mode OFF), the temperature was slowly increased, and the temperature dependence of $\chi_{\text{M}}T$ was recorded. $\chi_{\text{M}}T$ remains nearly constant as T increases from 10 K up to 70 K. The $\chi_{\text{M}}T$ value at 70 K is $0.61 \text{ cm}^3 \text{ K mol}^{-1}$, corresponding to about 17 % of HS molecules, then drops rapidly as the temperature is further increased, and reaches a value close to zero around 80 K. The critical LIESST temperature may then be defined as $T_{\text{liesst}} \approx 80 \text{ K}$ for the $\text{Fe}(\text{PM-BiA})_2(\text{NCS})_2$ in phase I. For $\text{Fe}(\text{PM-BiA})_2(\text{NCS})_2$ in phase II and $\text{Fe}_{0.216}\text{Mn}_{0.784}(\text{PM-BiA})_2(\text{NCS})_2$ the LIESST effect has also been observed at 10 K. The increase of the temperature reveals a critical value for the observation of the metastable HS state (T_{liesst}) around 50 K.

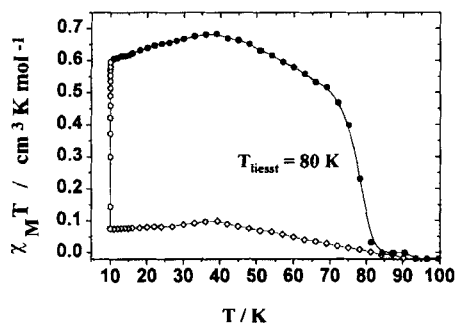


Figure 6. $\chi_{\text{M}}T$ versus T plots for $\text{Fe}(\text{PM-BiA})_2(\text{NCS})_2$ in phase I; ($\diamond \diamond \diamond$) without irradiation, ($o o o$) under irradiation at 10 K and ($\bullet \bullet \bullet$) under irradiation.

LITH effect

Recently, we have described for the first time a new type of bistability under irradiation on the phase I of $\text{Fe}(\text{PM-BiA})_2(\text{NCS})_2$.⁴ The same behavior has been also reported by Varret and coworkers on $[\text{Fe}_x\text{Co}_{1-x}(\text{btr})_2(\text{NCS})_2] \cdot \text{H}_2\text{O}$ with $x = 0.3, 0.5$ and 0.85 .¹⁸ We have called this phenomenon the LITH effect

(Light Induced Thermal Hysteresis).⁴ Figure 7 shows the magnetic behavior of $\text{Fe}(\text{PM-BiA})_2(\text{NCS})_2$ in phases I and II and $\text{Fe}_{0.216}\text{Mn}_{0.784}(\text{PM-BiA})_2(\text{NCS})_2$. This figure shows that for the three compounds a LITH effect is observed. The temperature dependence of $\chi_{\text{M}}T$ under irradiation (in mode ON) is rather similar to that in mode OFF when the temperature is increased from 10 K to 100 K (figures 7 and 6). The temperature dependence of $\chi_{\text{M}}T$ when cooling the sample in mode ON reveals a new type of hysteresis. For instance for the phase I, the HS molar fraction remains close to zero as T is lowered down to 60 K, then progressively increases as T is further lowered down to 10 K, and eventually reaches 20 %. It follows that the two curves in mode ON in the warming and cooling regime, respectively, show a bistability.

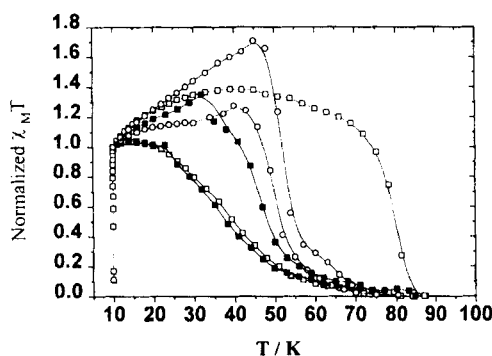


Figure 7. Magnetic properties recorded under light irradiation for (□ □ □) in phase I, (○ ○ ○) in phase II and (■ ■ ■) for $\text{Fe}_{0.216}\text{Mn}_{0.784}(\text{PM-BiA})_2(\text{NCS})_2$.

HS → LS relaxation

Figures 8 and 9 present the dynamics of the LIESST effect for $\text{Fe}(\text{PM-BiA})_2(\text{NCS})_2$ in phases I and II and for $\text{Fe}_{0.216}\text{Mn}_{0.784}(\text{PM-BiA})_2(\text{NCS})_2$. In phase I, the HS → LS relaxation is rather slow in the 5 - 78 K temperature range, and the time dependence of $\chi_{\text{M}}T$ can be studied with the SQUID setup. The decay of the HS molar fraction, γ_{HS} , versus time at various temperatures is represented in Figure 8. An analysis of these data indicates that the relaxation curves can be satisfactorily fitted with an Arrhenius law up to 60 K, while deviations from single exponential behavior are observed at higher temperatures ($60 < T < 80$ K); the time dependence of the HS molar fraction then follows a sigmoidal-type behavior.

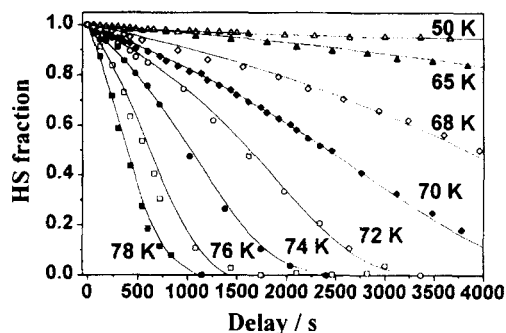
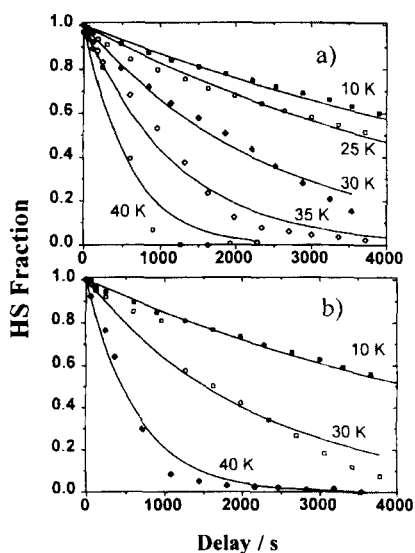


Figure 8. Time dependence at different temperatures of the HS molar fraction for the phase I.

For the phase II and $\text{Fe}_{0.216}\text{Mn}_{0.784}(\text{PM-BiA})_2(\text{NCS})_2$, the time dependence can be studied only until 40 K (figure 9). The relaxation curves can be satisfactorily fitted with an Arrhenius law. It is well established that the HS \rightarrow LS relaxation for spin transition compounds in the solid state is strongly influenced by cooperative effects.¹⁹ Hauser demonstrated by optical spectroscopy that in the highly diluted single crystal $[\text{Fe}_x\text{Zn}_{1-x}(\text{ptz})_6](\text{BF}_4)_2$ ($x = 0.1$) the γ_{HS} versus T curves followed first order kinetics, whereas for pure $[\text{Fe}(\text{ptz})_6](\text{BF}_4)_2$ compound sigmoidal relaxation curves were found. Such curves can be



interpreted as a self-acceleration of the HS \rightarrow LS relaxation as γ_{HS} decreases. Each HS ion in a crystal acts as internal pressure ("lattice pressure") and increases the relaxation rate. This "lattice pressure" is caused by the large reduction in size of the spin-crossover compound as it converts from HS to LS.¹⁹

Figure 9. Time dependence at various temperatures of the HS molar fraction a) for the phase II and b) for the $\text{Fe}_{0.216}\text{Mn}_{0.784}(\text{PM-BiA})_2(\text{NCS})_2$.

The result recorded for the $\text{Fe}(\text{PM-BiA})_2(\text{NCS})_2$ is in perfect agreement with Hauser's observations; a sigmoidal relaxation is measured for the phase I, which presents an abrupt spin transition (highly cooperative system), whereas an exponential behavior is observed for the phase II, where a gradual spin conversion occurs (weakly cooperative system). Nevertheless, according to the previous work performed on $[\text{Fe}(\text{ptz})_6](\text{BF}_4)_2$ and $[\text{Fe}_x\text{Zn}_{1-x}(\text{ptz})_6](\text{BF}_4)_2$, a faster HS \rightarrow LS relaxation rate is expected for the phase I due to the sigmoidal behavior. Our findings point out that the relaxation rate strongly depends on the crystal structure.

CONCLUSIONS

Phase I of $\text{Fe}(\text{PM-BiA})_2(\text{NCS})_2$ exhibits an exceptionally abrupt thermally-induced spin transition, whereas phase II and doped compounds show gradual conversions. The EPR spectra reveals that the structure of the two phases of $\text{Fe}(\text{PM-BiA})_2(\text{NCS})_2$ are totally different. A pronounced change in the LIESST behavior is also measured between the two phases. The rate of relaxation for the phase I is slower than for the phase II. Recently, we have suggested that the slow rate of relaxation of the phase I was due to an unusually large change in Fe-N bond lengths between LS and HS states. The LIESST data indicate that the modification of the FeN_6 core is more pronounced for the phase II than for the phase I.

References

- [1] H. A. Goodwin, *Coord. Chem. Rev.*, **18**, 293 (1976) ; P. Gülich, *Struct. Bonding (Berlin)*, **44**, 83 (1981); E. König, *Prog. Inorg. Chem.*, **35**, 527 (1987); P. Gülich and A. Hauser, *Coord. Chem. Rev.*, **97**, 1 (1990) ; E. König, *Struct. Bonding (Berlin)*, **76**, 51 (1991); P. Gülich, A. Hauser, H. Spiering, *Angew. Chem. Int. Ed. Engl.*, **33**, 2024 (1994); P. Gülich, J. Jung, H. Goodwin, *Molecular Magnetism : From Molecular Assemblies to the Devices*, Eds. Coronado et al. 327 (1996).
- [2] O. Kahn, J. P. Launay, *Chemtronics*, **3**, 140 (1988); O. Kahn, *Molecular Magnetism*, VCH, New York (1993); O. Kahn, J. Kröber, C. Jay, *Adv. Mater.*, **4**, 718 (1992).
- [3] J.-F. Létard, P. Guionneau, E. Codjovi, O. Lavastre, G. Bravic, D. Chasseau, O. Kahn, *J. Amer. Chem. Soc.*, **119**, 10861 (1997).
- [4] J.-F. Létard, P. Guionneau, L. Rabardel, J.A. K. Howard, A.E. Goeta, D. Chasseau, O. Kahn, *Inorg. Chem.*, **37**, 4432 (1998).
- [5] J.-F. Létard, S. Montant, P. Guionneau, P. Martin, A. Le Calvez, E. Freysz, D. Chasseau, R. Lapouyade, O. Kahn, *J. Chem. Soc. Chem. Comm.*, 745 (1997).
- [6] P. Guionneau, J.-F. Létard, D.S. Yufit, D. Chasseau, G. Bravic, A.E. Goeta, J.A.K. Howard, O. Kahn, *J. Mater. Chem.*, submitted.

- [7] Y. Servant, C. Cantin, O. Kahn, J. Kliava, in: First Asia-Pacific EPR/ESR Symposium, Hong Kong (1997), C.Z. Rudowicz ed., Springer-Verlag, 346 (1998).
- [8] W. Vreugdenhil, J.G. Haasnoot, O. Kahn, P. Thuery, J. Reedjik, *J. Am. Chem. Soc.*, **109**, 5272 (1987); W. Vreugdenhil, J.H. Van Diemen, R.A.G. De Graaff, J.G. Haasnoot, J. Reedjik, A.M. Van der Kraam, O. Kahn, J. Zarembowitch, *Polyhedron*, **9**, 2971 (1990).
- [9] C. Cantin, J. Kliava, Y. Servant, L. Sommer, O. Kahn, *Appl. Magn. Reson.*, **12**, 81 (1997); *ibid.*, **12**, 87 (1997).
- [10] A. Ozarowski, B.R. McGarvey, A.B. Sarkar, J.E. Drake, *norg.Chem.*, **7**, 628 (1988); A. Ozarowski, B.R. McGarvey, *Inorg.Chem.*, **28**, 2262 (1989).
- [11] A. Ozarowski, Y. Shunzhong, B.R. McGarvey, A. Mislankar, J.E. Drake, *Inorg.Chem.*, **30**, 3167 (1991).
- [12] P.S. Rao, A. Reuveni, B.R. McGarvey, P. Ganguli, P. Gütllich, *Inorg. Chem.*, **20**, 204 (1981).
- [13] P.E. Doan, B.R. McGarvey, *Inorg. Chem.*, **29**, 874 (1990).
- [14] H. Daubric, C. Cantin, C. Thomas, J. Kliava, J.-F. Létard, O. Kahn, *J. Chem. Phys.*, submitted.
- [15] J. Kliava, *Phys. Stat. Sol. B*, **134**, 411 (1986).
- [16] G. L. Bir, *Soviet Physics – Solid State*, **5**, 1628 (1964).
- [17] S. Decurtins, P. Gütllich, C.P. Köhler, H. Spiering, A. Hauser, *Chem. Phys. Lett.*, **105**, (1984); S. Decurtins, P. Gütllich, K.M. Hasselbach, A. Hauser, H. Spiering, *norg.Chem.*, **24**, 2174 (1985).
- [18] A. Desaix, O. Roubeau, J. Jęftic, J. Haasnoot, K. Boukheddaden, E. Codjovi, J. Linarès, M. Noguès, F. Varret, *Eur. Phys. J. B*, **000** (1998).
- [19] A. Hauser, *Chem. Phys. Lett.*, **124**, 543 (1986); *192* 65 (1992); R. Hinek, P. Gütllich, A. Hauser, *Inorg. Chem.*, **33**, 567 (1994); R. Hinek, H. Spiering, P. Gütllich, A. Hauser, *Chem. Eur.J.*, **2**, 1435 (1996).